Journal of Catalysis **183,** 281–291 (1999)
Article ID jcat.1999.2394, available online at http://www.idealibrary.com on IDEAL®

Synthesis, Characterization, and Catalytic Properties of Mesoporous Tin-Containing Analogs of MCM-41

K. Chaudhari,* T. K. Das,* P. R. Rajmohanan,* K. Lazar,† S. Sivasanker,* and A. J. Chandwadkar*,[1]

*National Chemical Laboratory, Pune, 411008, India; and †Institute of Isotopes, Budapest, Hungary

Received August 5, 1998; revised December 24, 1998; accepted December 26, 1998

Mesoporous stannosilicate molecular sieves with the MCM-41 structure have been synthesized by hydrothermal methods and characterized in detail by elemental analysis, XRD, N_2 adsorption measurements, and UV–visible, IR, ^{13}C CP/MAS NMR, ^{29}Si MAS NMR, ^{119}Sn MAS NMR, and Mössbauer spectroscopic methods. The increase in the unit-cell parameter (XRD), the presence of an absorption band at ~208 nm (UV–vis), and Mössbauer spectroscopy suggest the incorporation of Sn into the MCM-41 structure. The Sn-MCM-41 samples catalyze the selective oxidation/epoxidation of organic compounds by aqueous H_2O_2/tertiary butyl hydroperoxide.

INTRODUCTION

Mesoporous molecular sieves designated as M41S have attracted the attention of many researchers since their discovery at Mobil Oil Corporation (1, 2). These materials possess well-defined mesopores the diameters of which can be tailored to the desired value (18–100 Å) by the proper choice of surfactants, auxiliary organics, and synthesis parameters. Since the discovery of MCM-41 (a member of the M41S family) possessing a hexagonal array of uniform pores, several reports have appeared on the isomorphous substitution of Si by other elements such as Ti (3–5), vanadium (6–8), Sn [a Short Communication by us (9)], chromium (10, 11), and zirconium (12). The above isomorphs were also active as catalysts for the selective oxidation of organic molecules under mild conditions.

Substitution of aluminum by tin in the faujasites, mordenites, and ZSM-5 by postsynthesis (13–16) or by hydrothermal crystallization (17, 18) and of silicon in Sn-silicalite-1 (19) and Sn-silicalite-2 (20) is known. Sn-silicalite-1 and Sn-silicalite-2 (medium-pore zeolites) are catalytically active in the hydroxylation of small molecules such as phenol and cresol.

In this paper, we report the hydrothermal synthesis, physicochemical properties, and catalytic activities of a tin-containing analog of MCM-41 (Sn-MCM-41).

[1] To whom correspondence should be addressed. Fax: +91–020–393761. E-mail: asha@cata.ncl.res.in.

EXPERIMENTAL

Materials

The syntheses of Si-MCM-41 and Sn-MCM-41 were carried out hydrothermally using fumed silica (99%, Sigma), tetramethylammonium silicate (TMA silicate; 10 wt% silica solution, $TMA/SiO_2 = 0.5$; Sachem Inc., USA), cetyltrimethylammonium chloride/hydroxide (CTMACl/OH; 17.9 wt% Cl, 6.7 wt% OH) prepared in the laboratory by partial exchange of CTMACl (25 wt% aqueous solution, Aldrich) over an ion-exchange resin, tetramethylammonium hydroxide (TMAOH; 99%, Aldrich), and stannic chloride ($SnCl_4 \cdot 5H_2O$; 98%, Loba Chemie, Bombay, India).

Synthesis of Si-MCM-41

The molar composition of the synthesis gel in terms of oxides was as follows: $SiO_2 : 0.086(NH_4)_2O : 0.089(CTMA)_2O : 0.155(TMA)_2O : 40H_2O$. Ammonium hydroxide (1.8 g, 25% solution) diluted with water (12.5 g) was added to a solution of cetyltrimethylammonium chloride/hydroxide (16.7 g, 24.6% solution, Aldrich) with stirring. To this mixture, 2.08 g TMAOH dissolved in 12.5 g water was added followed by the addition of 13.6 g TMA silicate. The thick gel formed was stirred for 20 min. Next, fumed silica (3.1 g) was added slowly to the above gel under stirring and the mixture stirred further for 1 h. The pH of the final gel was 11.5. The gel was then transferred to a stainless-steel autoclave and heated in an air oven at 383 K for 4 days for crystallization. After the crystallization, the product was filtered, washed with deionized water, and dried at 373 K for 5 h. The product was finally calcined at 823 K for 3 h in nitrogen and then for 6 h in air.

Synthesis of Sn-MCM-41

The molar composition of the synthesis gel in terms of oxides was as follows: $SiO_2 : 0–0.02SnO_2 : 0.089(CTMA)_2O : 0.155(TMA)_2O : 40H_2O$. In a typical synthesis, 0.52 g $SnCl_4 \cdot 5H_2O$ (for $Si/Sn = 50$) was dissolved in 15 g water and added to 16.7 g of a 24.6% solution of CTMACl/

0021-9517/99 $30.00

OH with stirring. To this stirred mixture, 2.08 g TMAOH dissolved in 10 g water and 13.6 g TMA silicate were added. The thick gel formed was stirred further for 15 min. Fumed silica (3.1 g) was then added slowly in about 10 min to the above solution under stirring and the stirring was continued for 1 h after completion of addition. The mixture was transferred to a stainless-steel autoclave and heated at 383 K for 5 days. The solid material was then filtered, washed with deionized water, and dried at 373 K in air. The product was calcined at 823 K in flowing nitrogen (for 3 h) and in flowing air (for 6 h) to remove the organic material. A total of four samples of different Sn contents [designated Sn-MCM-41(A), Sn-MCM-41(B), Sn-MCM-41(C), and Sn-MCM-41(D) with Si/Sn = 178, 133, 83, and 42, respectively] were prepared following the general synthesis procedure described above using different quantities of tin tetrachloride $SnCl_4 \cdot 5H_2O$.

Synthesis of Sn-Silica Gel

Sn-silica gel was prepared for comparison of its catalytic activity with Sn-MCM-41 samples. Sn-silica gel (Si/Sn = 50) was synthesized by adding fumed silica (1.55 g) to TMA silicate solution (6.8 g) with stirring; then $SnCl_4 \cdot 5H_2O$ (0.26 g) dissolved in water (15.0 g) was added and the mixture was stirred for some time. The gel obtained was dried at 823 K for 6 h.

Characterization

The chemical compositions of the samples were determined by a combination of wet chemical methods and atomic absorption spectrometry (Hitachi, Model Z 800). XPS measurements were carried out using a V. G. Scientific ESCA-3-MK II X-ray photoelectron spectrometer with Al$K\alpha$ X-ray source. The binding energy values were measured with reference to the carbon peak at 285.0 eV.

The crystalline phase identification and phase purity determination of the as-synthesized and calcined samples were carried out by XRD (Philips, Holland) using nickel-filtered Cu$K\alpha$ radiation, ($\lambda = 1.5406$ Å).

The sorption capacities for H_2O, *n*-hexane, and benzene were measured using a vacuum (Cahn, USA) electrobalance. Prior to sorption measurements, about 200 mg of the sample was activated at 673 K under vacuum. The surface areas and pore diameters were determined from N_2 adsorption isotherms using a Coulter (Omnisorp 100 CX) instrument.

The UV–vis diffuse reflectance spectra of the samples were obtained using a Shimadzu (Model UV-2101 PC) spectrometer. Fourier transform infrared (FTIR) spectra were recorded using a Nicolet FTIR spectrometer (Model 60 × B) with KBr pellets.

The NMR spectroscopic studies were carried out on a Bruker MSL 300 NMR spectrometer. The resonance frequencies of ^{119}Sn, ^{13}C, and ^{29}Si were 111.8, 75.5, and 59.6 MHz, respectively. For the magic-angle spinning (MAS) NMR studies, the finely powdered samples were placed in 7.0-mm-o.d. zirconia rotors and spun at 2.5–3.3 kHz. For the ^{13}C CP/MAS experiments, the Hartmann–Hahn match conditions were adjusted using adamantane. The ^{13}C signal of the CH_2 carbon of adamantane was taken as a secondary reference ($\delta = 28.7$ ppm from TMS). The ^{119}Sn signals were referred to the isotropic peak of SnO_2 taken as $\delta = -604$ ppm (with respect to tetramethyl tin). Tetraethyl orthosilicate ($\delta = 82.4$ ppm from TMS) was used as the reference compound for ^{29}Si.

Mössbauer spectra were recorded on three tin-containing MCM-41 analogs, denoted Sn-MCM-41(B), Sn-MCM-41(C), and Sn-MCM-41(D) at 77 and 300 K. Two series of measurements were performed. In the first series, the spectra of the three samples were recorded in the calcined state at two temperatures. In the second series, *in situ* spectra were obtained on a selected sample [Sn-MCM-41(C)] to study the effects of reduction (670 K for 2 h in H_2 flow) and oxidation (520 K for 2 h in flow of air) on the state of tin. The isomer shift values reported are relative to SnO_2 at 300 K. For the deconvolution, a Lorentzian line shape was assumed and none of the positional parameters was constrained. The estimated accuracy of positional data is ±0.03 mm/s.

Catalytic activity tests were carried out using a batch reactor at atmospheric pressure (at 353 K). Aqueous H_2O_2 (25 wt% solution) was used in the hydroxylation of phenol and 1-naphthol while tertiary butyl hydroperoxide (TBHP, 70% aqueous solution, Aldrich) was used in the epoxidation of norbornene. In a standard run of phenol hydroxylation, 1 g phenol, 10 g water, and 0.1 g catalyst were taken in a 50 ml-round-bottom flask equipped with a condenser and heated at 353 K in an oil bath with stirring. H_2O_2 was added (phenol/H_2O_2 mole ratio = 3) to the reaction mixture and the reaction was continued for 24 h. The oxidation of 1-naphthol was carried out by taking 0.5 g reactant, 10 g acetonitrile, and 0.1 g catalyst in a 50-ml round-bottom flask attached to a condenser and heated at 353 K in an oil bath. The oxidant (H_2O_2) was added to the reaction mixture and the reaction was carried out for 24 h. In the epoxidation of norbornene, 0.5 g of norbornene dissolved in 10 g of acetonitrile was taken in a 50-ml round-bottom flask and 0.1 g of the catalyst was added to it. TBHP (norbornene/TBHP = 1.5) was added to the above mixture. The reaction was continued for 24 h, and the product removed from the flask at different intervals. The products were analyzed by GC (HP-5880A) equipped with a methyl-silicon gum capillary column (HP1, 50 m long and 0.2 mm i.d.) and a flame ionization detector.

RESULTS AND DISCUSSION

Chemical Analysis

The results of the chemical analysis of the Si-MCM-41 and Sn-MCM-41 samples are presented in Table 1.

TABLE 1

Composition and Physicochemical Characteristics of the Samples

Sample	SiO_2/SnO_2 (mole ratio)			XRD d_{100} (Å)	Unit-cell parameter, a_0 (Å)	BET surface area[a] (m^2/g)	Pore diameter (Å)
	Gel	Product					
		Chemical analysis	XPS				
Si-MCM-41	∞	∞	∞	36.77	42.5	975	27.0
Sn-MCM-41(A)	200	178	176	38.38	44.31	978	28.5
Sn-MCM-41(B)	150	133	129	39.39	45.48	990	29.6
Sn-MCM-41(C)	100	83	81	39.58	45.70	1031	30.2
Sn-MCM-41(D)	50	42	42	39.66	45.80	1082	30.5
Sn-impregnated MCM-41	—	50	48	—	—	—	—
Sn-silica gel[b]	50	50	47	—	—	—	—

[a] Calculated from N_2 adsorption isotherm at liquid nitrogen temperature.
[b] Amorphous sample for comparison (see Experimental).

The chemical compositions determined by chemical analysis and XPS analysis are similar. X-ray photoelectron spectra of the samples show typical doublets for Sn $3d_{3/2}$ and $3d_{5/2}$ electrons with binding energies of 496.3 and 488.0 eV, respectively (20), indicating the presence of Sn^{4+} at the surface. The surface chemical compositions were calculated from the intensities of the Sn 3*d* and Si 2*s* peaks (20) and are given in Table 1. The good correspondence between the compositions from chemical and XPS methods confirms that the Sn^{4+} ions are uniformly distributed in the surface and the bulk in the samples. Further, no loss of Sn occurred on extraction with dilute HCl (1 : 10), suggesting the absence of Sn^{2+} ions in the samples.

XRD

The XRD patterns of the calcined Sn-MCM-41 samples with different Si/Sn ratios [Sn-MCM-41(A), Sn-MCM-41(B), Sn-MCM-41(C), Sn-MCM-41(D)] and the pure silica Si-MCM-41 are given in Fig. 1. The samples produce relatively well-defined XRD patterns, with one major peak along with three small peaks identical to those of MCM-41 materials (1, 2). Beck *et al.* (2) indexed these peaks for a hexagonal unit cell, the parameter of which was calculated from the equation $a_0 = 2d_{100}/\sqrt{3}$. The unit-cell parameter and *d* spacing of the Sn-MCM-41 samples and Si-MCM-41 are given in Table 1. The slight increase in *d* spacing and unit-cell parameter of Sn-MCM-41 compared with its pure silica analog (Table 1) suggests the presence of tin in the framework. The increase in unit-cell parameter on Sn incorporation is probably due to the larger size of Sn^{4+} (radius, 0.55 Å) compared with Si^{4+} (radius, 0.26 Å). It is also observed that the unit-cell parameter increases with increasing Sn content. A similar increase was observed by earlier workers with MCM-41 containing aluminum (2, 21), titanium (3), and vanadium (6).

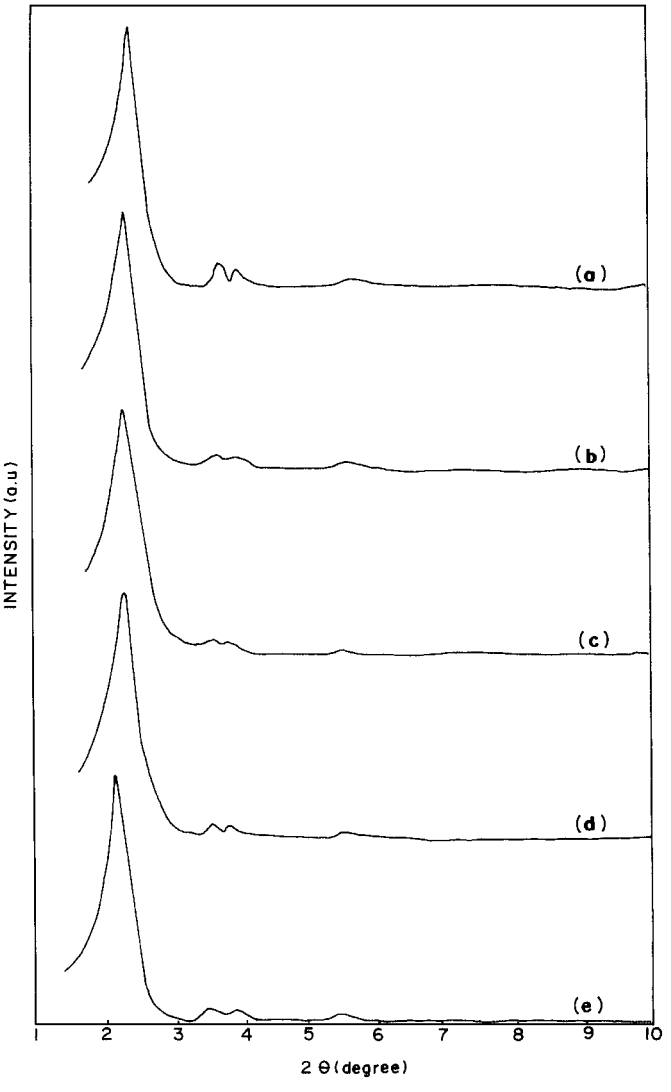

FIG. 1. XRD patterns of calcined (a) Si-MCM-41, (b) Sn-MCM-41(A), (c) Sn-MCM-41(B), (d) Sn-MCM-41(C), and (e) Sn-MCM-41(D).

TABLE 2

Adsorption Capacity and Pore Volume of the Samples

Sample	Sorption capacity (mass %)[a]			Pore volume (ml/g)		
	H_2O	*n*-Hexane	Benzene	*n*-Hexane	Benzene	N_2[b]
Si-MCM-41	13.8	45.10	56.1	0.684	0.642	0.631
Sn-MCM-41(A)	15.7	46.70	58.03	0.709	0.664	—
Sn-MCM-41(B)	17.53	47.02	60.52	0.713	0.692	0.664
Sn-MCM-41(C)	19.50	49.2	62.42	0.747	0.714	—
Sn-MCM-41(D)	20.1	50.3	63.1	0.763	0.722	0.733

[a] Gravimetric adsorption (Cahn electrobalance) at $p/p_0 = 0.5$ and 298 K.

[b] Calculated from N_2 adsorption isotherm at liquid nitrogen temperature.

Sorption

The N_2 adsorption isotherms of the samples revealed a uniform pore size. The average pore diameters calculated from N_2 adsorption isotherms using the BJH model (22) are presented in Table 1. The above model was chosen as it has been derived for nonintersecting cylindrical pores (23) as in MCM-41-type materials. However, as the model uses the Kelvin equation, the validity of which is questionable for pores of diameter less than 50 Å (22), systematic errors might be present in the estimated pore diameters (Table 1). However, the reported trend in the pore diameters for the different samples is expected to be the same. The pore diameters increase with increasing Sn content of the samples. The pore volumes calculated (at $p/p_0 = 0.5$) from N_2, *n*-hexane, and benzene adsorption are similar (Table 2). The amounts of H_2O adsorbed are, however, smaller (24).

The UV-vis diffuse reflectance spectra of calcined Sn-MCM-41 samples reveal absorption at 208 ± 5 nm (Fig. 2). The intensity of this absorption band is observed to increase with increase in Sn content in the samples and reveals the presence of Sn^{4+} in tetrahedral coordination (19). In addition to this band, an additional band at ~230 nm is observed in the case of Sn-MCM-41(D) (Si/Sn = 50; Fig. 2), indicative of the presence of small amounts of hexacoordinated Sn species at high Sn contents. These observations are similar to those made by Mal and Ramaswamy in the case of Sn-MFI molecular sieves (19). For comparison, the spectra of pure SnO_2 and Sn-impregnated MCM-41 are also included in Fig. 2. Both Sn-impregnated MCM-41 and SnO_2 show broad absorption at 280 ± 5 nm which may be assigned to hexacoordinated polymeric Sn–O–Sn-type species.

FTIR

The framework IR spectra of the Si-MCM-41 and Sn-MCM-41 samples are presented in Fig. 3. The T–O–T lattice vibration is found to shift to lower wavenumbers for Sn-MCM-41, probably due to the incorporation of Sn in the lattice (20). The IR spectra show a band at 970 cm^{-1} and the intensity of this band increases with increasing Sn content. This band is generally considered a proof of the incorporation of the heteroatom into the framework. Camblor *et al.* (25) proposed that the band at 960 cm^{-1} is due to the Si–O stretching vibrations of Si–OH groups present at defect sites. This vibration has also been detected in Ti- and V-containing silica molecular sieves (26, 27).

^{13}C NMR

The ^{13}C CP/MAS NMR spectra of Sn-MCM-41, Si-MCM-41, and CTMACl are presented in Fig. 4. A comparison of the ^{13}C CP/MAS NMR spectra of the uncalcined MCM-41 and Sn-MCM-41 samples (Figs. 4a–4c) with that of $CTMA^+$ cations in solution (Fig. 4d) shows that $CTMA^+$ cations remain intact inside the pores of the molecular sieves. The ^{13}C NMR spectra of the $CTMA^+$ in solution and uncalcined Sn-MCM-41 are similar, except for minor changes in the chemical shifts and resolution. The maximum shift ($\delta = \sim 1.4$ ppm) is observed for the terminal methyl carbon. The methyl carbon is shifted to a higher field when the surfactant is in the zeolite channel. The peak at $\delta =$ 66 ppm can be assigned to the methylene carbon of the cetyl chain bonded to the nitrogen atom. The three methyl groups bonded to nitrogen atoms resonate at 53 ppm. The signals between 22 and 32 ppm are from the different

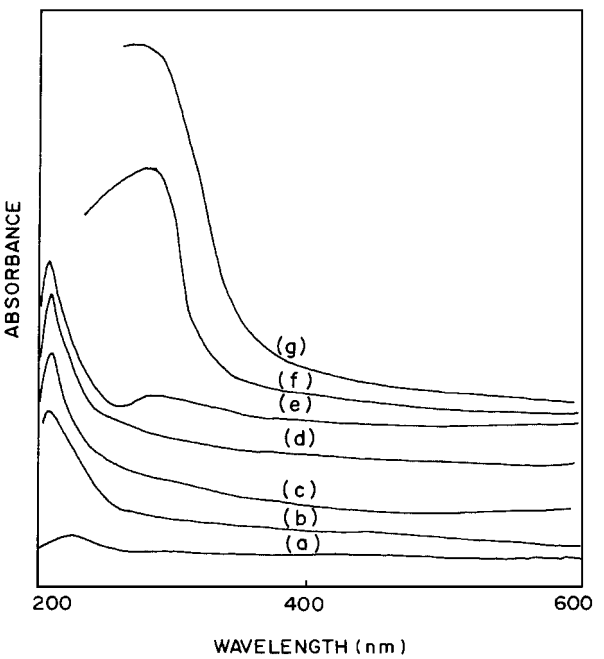

FIG. 2. Diffuse reflectance UV–vis spectra of calcined (a) Si-MCM-41, (b) Sn-MCM-41(A), (c) Sn-MCM-41(B), (d) Sn-MCM-41(C), (e) Sn-MCM-41(D), (f) Sn-impregnated MCM-41, and (g) SnO_2.

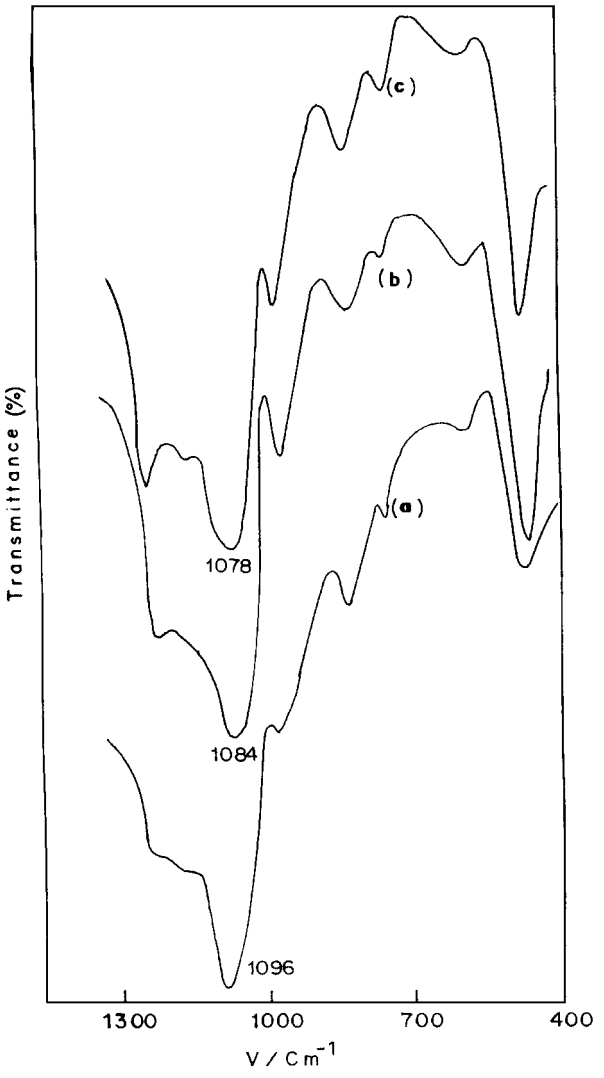

FIG. 3. Framework IR spectra of calcined (a) Si-MCM-41, (b) Sn-MCM-41(C), and (c) Sn-MCM-41(A).

methylene carbon atoms in the cetyl chain. A comparison of the ^{13}C CP/MAS NMR spectrum of Sn-MCM-41 (Figs. 4b and 4c) with that of Si-MCM-41 (Fig. 4a) reveals negligible peak broadening for the $=N-CH_2$ (at $\delta = 66$ ppm) and the $=N-CH_3$ (at $\delta = \sim 54$ ppm) carbons in the former sample when compared with the latter one. A broadening of these lines has been correlated by earlier workers with the negative charge on the framework of transition metal-incorporated MCM-41 (28). It therefore, appears that the incorporation of Sn occurs mainly as Sn^{4+} ions which do not change the charge on the framework unlike the incorporation of di- and trivalent metal cations such as Co and Fe.

^{29}Si MAS NMR

In Fig. 5, the ^{29}Si MAS spectra obtained for Sn-MCM-41 systems are compared with those of Si-MCM-41 in the as-synthesized (Figs. 5a–5c) and the calcined (Figs. 5d–5f) forms. The as-synthesized samples show two broad resonances with chemical shifts at $\delta = \sim -102$ and -112 ppm, which can be assigned, respectively, to the Q_3 and Q_4 silicon environments. The broadness of the ^{29}Si signals has been attributed to the large distribution of the TOT angles (2). It is evident from these spectra that tin substitution does not give rise to any additional ^{29}Si peaks. The lack of high sensitivity for ^{29}Si signals is indicative of the very long spin-lattice relaxation time associated with the MCM-41 system. Nevertheless, a comparison of the ^{29}Si MAS spectra recorded

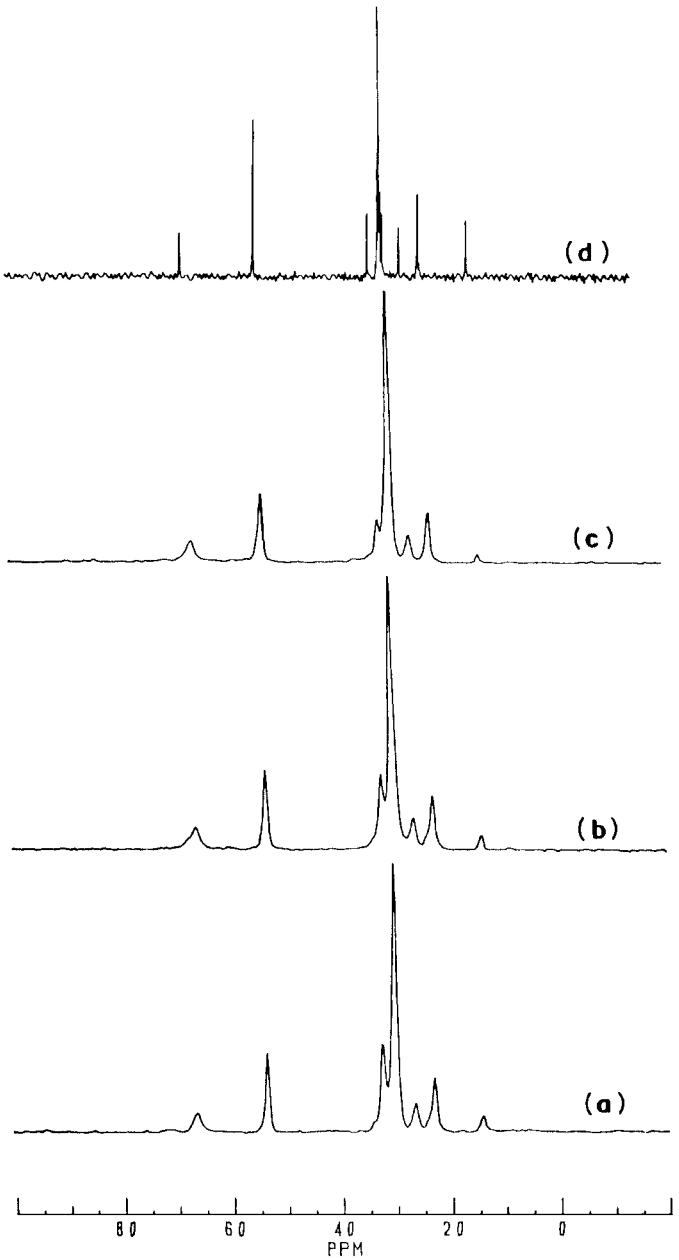

FIG. 4. ^{13}C CP/MAS NMR spectra of as-synthesized (a) Si-MCM-41, (b) Sn-MCM-41(C), (c) Sn-MCM-41(D), and (d) aqueous solution of $CTMA^+$ ions.

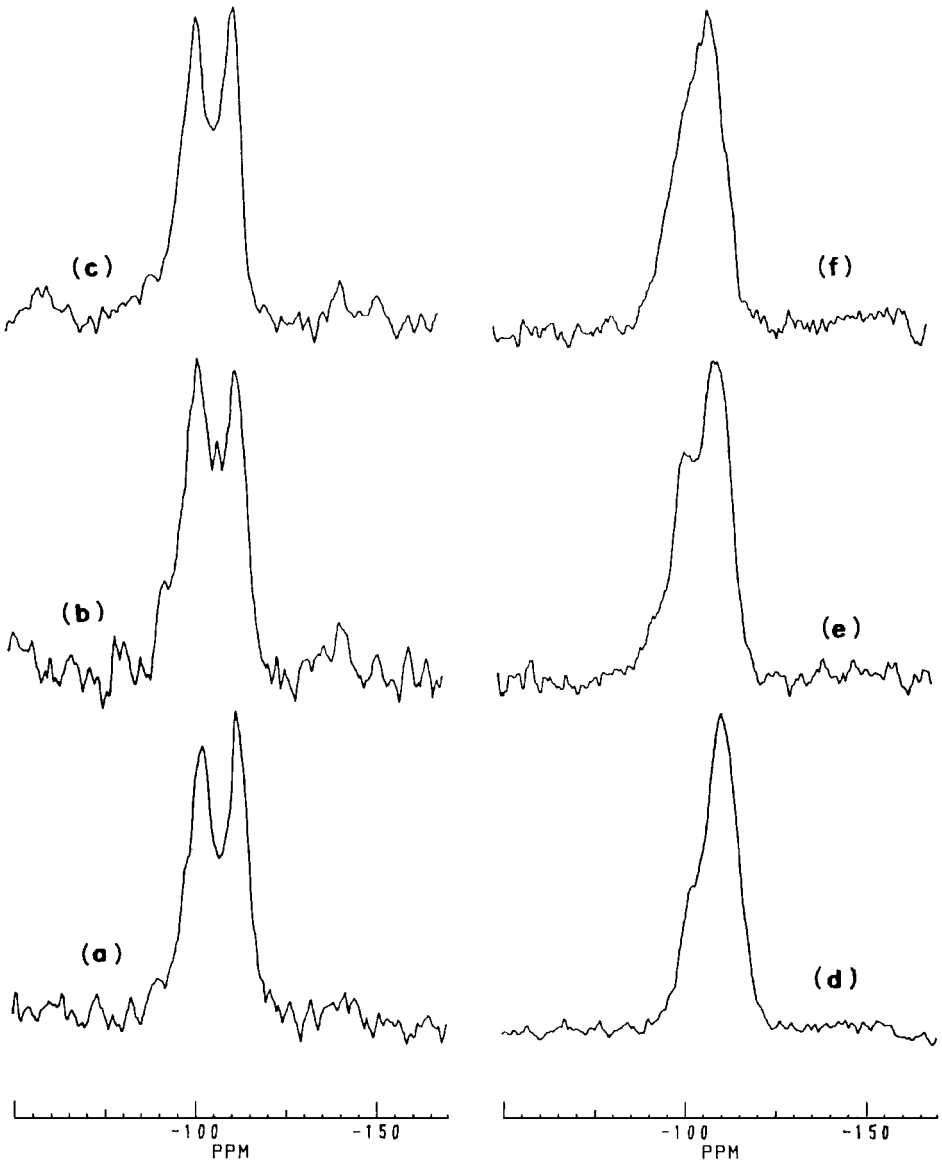

FIG. 5. ^{29}Si MAS NMR spectra of as-synthesized (a) Si-MCM-41, (b) Sn-MCM-41(C), and (c) Sn-MCM-41(D) and calcined (d) Si-MCM-41, (e) Sn-MCM-41(C), and (f) Sn-MCM-41(D).

under identical conditions for the as-synthesized samples (Figs. 5a–5c) indicates that the Q_3 signal at $\delta = \sim -102$ ppm is slightly more for the Sn samples than for the Si sample, in keeping with the larger surface areas of the former. As expected, due to dehydroxylation, the intensity of the Q_3 sites decreases on calcination of the samples (Figs. 5c and 5d).

^{119}Sn MAS NMR

Though the natural abundance and the magnetogyric ratio of ^{119}Sn are higher than those of ^{29}Si, the detection of Sn in stannosilicates is not easy due to the low incorporation, long spin-lattice relaxation times, and, to some extent, the large chemical shift anisotropy (CSA). Nevertheless, an attempt has been made to record the static and MAS spectra of Sn-MCM-41 samples, the results of which are presented in Fig. 6. The ^{119}Sn spectrum of pure SnO_2 (static) (Fig. 6a) and a 5% (w/w) mixture of SnO_2 in Si-MCM-41 (Fig. 6d) are also presented for comparison. The overall sensitivity of ^{119}Sn in Sn-MCM-41 is low, especially under magic-angle spinning conditions. The better sensitivity obtained for the samples recorded in the static mode than under MAS conditions is due to the large amount of sample (∼four times) that could be accommodated in the sample tube (10 mm o.d., ∼5 cm length) in the static measurements. Isotopic chemical shifts of $\delta = \sim -677$ ppm and $\delta = -710$ ppm are observed for Sn-MCM-41(C) and Sn-MCM-41(D), respectively. Under the same experimental conditions, octahedrally

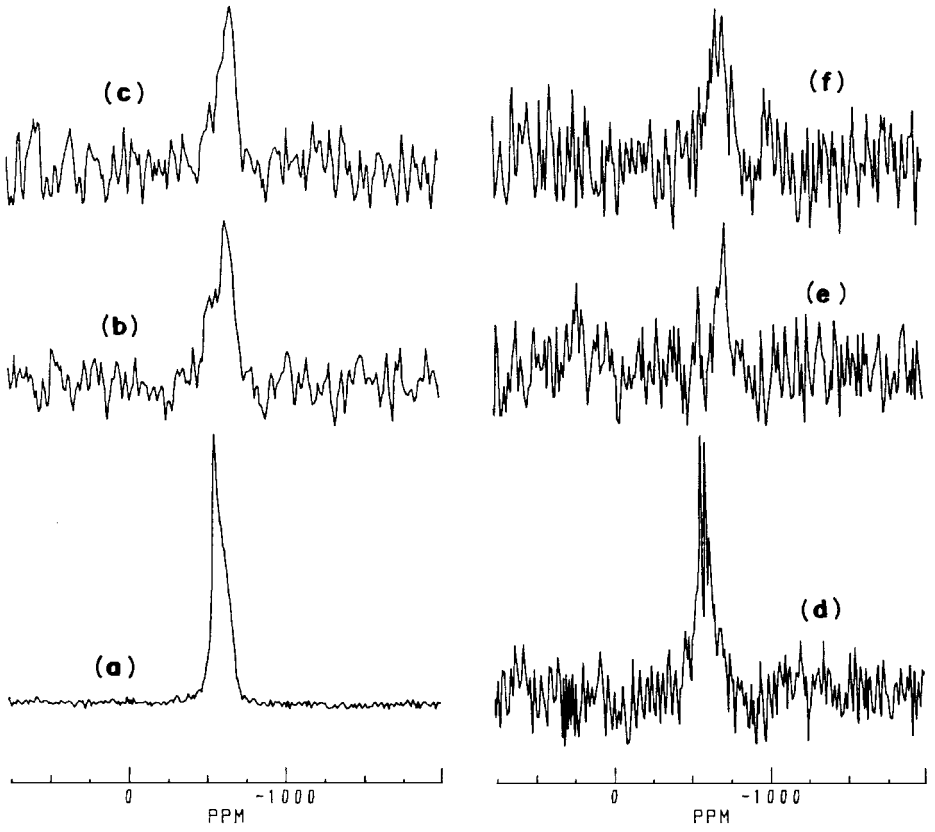

FIG. 6. ^{119}Sn static NMR spectra of (a) SnO_2, (b) Sn-MCM-41(C), and (c) Sn-MCM-41(D) and MAS NMR spectra of (d) 5% (w/w) mixture of SnO_2 and Si-MCM-41, (e) Sn-MCM-41(C), and (f) Sn-MCM-41(D).

coordinated tin in pure SnO_2 shows a chemical shift of $\delta = -604$ ppm (Fig. 6d). Thus, the chemical shift values obtained for Sn-MCM-41 samples can be attributed to the tetrahedral coordination of the Sn^{4+} ions.

Mössbauer Spectroscopy

The Mössbauer spectra of the tin-containing samples [Sn-MCM-41(B), Sn-MCM-41(C), and Sn-MCM-41(D)] are shown in Fig. 7 and the parameters obtained from the corresponding fits are collected in Table 3. Besides the regular Mössbauer parameters [isomer shift (IS) and quadrupole splitting (QS), respectively] the corresponding $d\ \ln(A_{300}/A_{77})/dT$ values were also determined (A is the spectral area of the given component relative to the baseline at 300 K or 77 K).

The sample Sn-MCM-41(C) exhibiting the largest $d\ \ln(A_{300}/A_{77})/dT$ value was selected for further *in situ* reduction/oxidation studies. Spectra obtained after 670 K reduction and 520 K calcination are shown in Fig. 8 and the corresponding IS, QS, and $d\ \ln A/dT$ values are presented in the bottom of Table 3.

Samples Sn-MCM-41(B) and Sn-MCM-41(C) exhibit rather low isomer shift values (close to −0.2 mm/s). Similar IS values were reported on tin-containing zeolites (29, 30). This low value is probably characteristic of tetrahedrally coordinated Sn^{4+}. For this assignment it may be recalled that the value of the isomeric shift of tin is a result of contributions from *p* and *s* electrons. An increase in the *p* symmetry results in a decrease in the isomer shift. Compared with octahedral bonding as in SnO_2 (31), tetrahedral bonding requires a larger contribution from *p* electrons. Thus, it appears that the Sn ions in Sn-MCM-41(B) and Sn-MCM-41(C) are present mostly in tetrahedral coordination,

TABLE 3

Mössbauer Parameters of the Samples

		300 K		77 K		$-d\ \ln(A_{300}/A_{77})/dT \times 10^{-2}$
		IS	QS	IS	QS	
Sn-MCM-41(B)	Sn^{4+}	−0.24	0.22	−0.21	0.31	0.665
Sn-MCM-41(C)	Sn^{4+}	−0.26	0.37	−0.21	0.32	0.863
Sn-MCM-41(D)	Sn^{4+}	−0.10		−0.09	0.47	0.496
Sn-MCM-41(C)						
Calcined	Sn^{4+}	−0.26	0.37	−0.21	0.32	0.863
670 K/H_2	Sn^{4+}			−0.21	0.33	0.783
	Sn^{2+}			2.77	1.95	1.22
520 K/air	Sn^{4+}	−0.12	0.56	−0.10	0.57	0.627

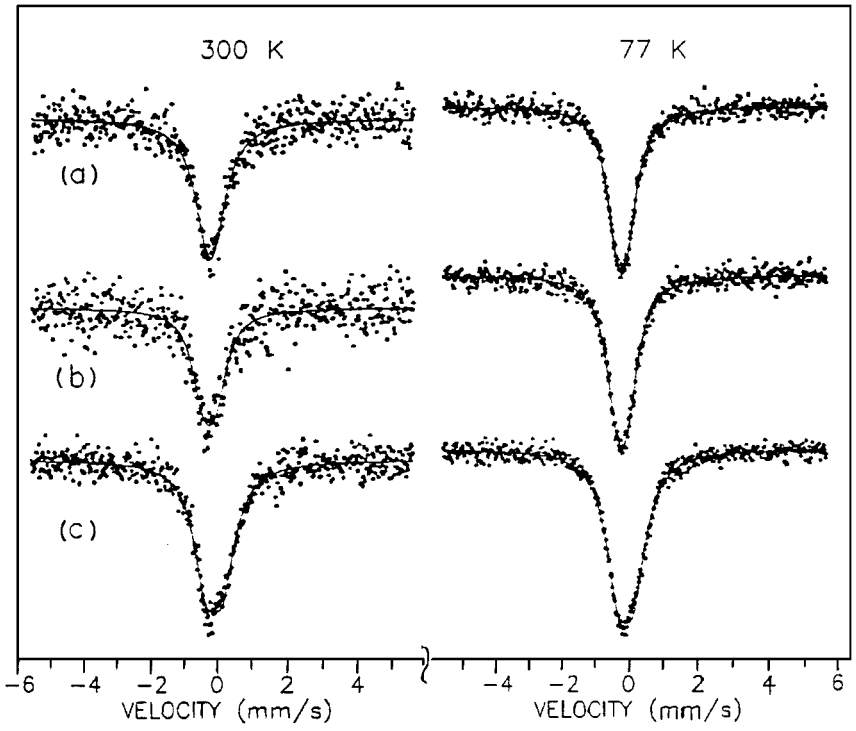

FIG. 7. ^{119}Sn Mössbauer spectra of Sn-MCM-41 samples at 300 and 77 K: (a) Sn-MCM-41(B), (b) Sn-MCM-41(C), (c) Sn-MCM-41(D).

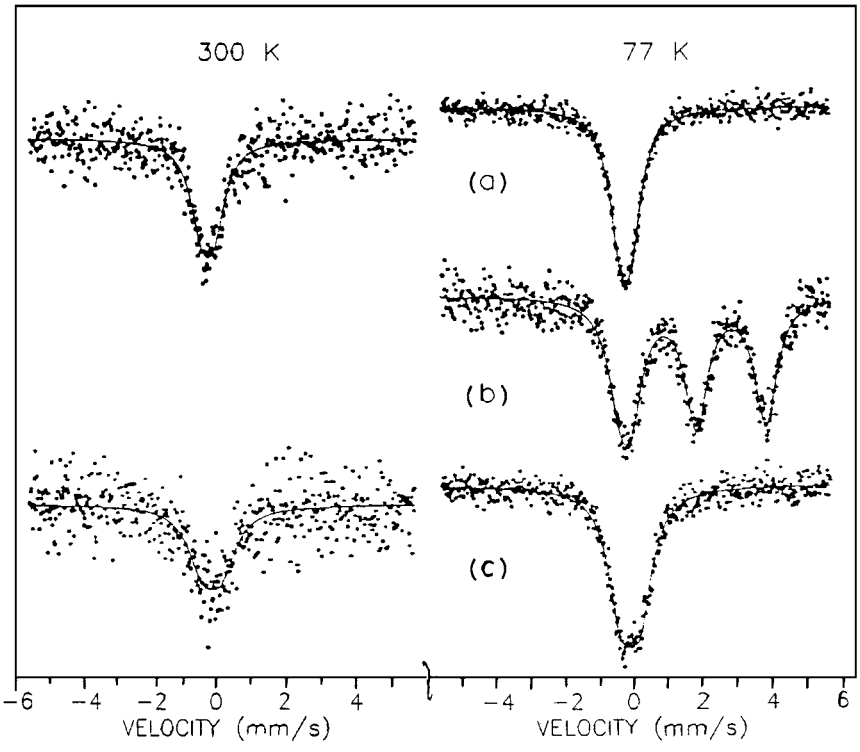

FIG. 8. *In situ* ^{119}Sn Mössbauer spectra obtained on (a) Sn-MCM-41(C), (b) Sn-MCM-41(C) treated in hydrogen at 670 K for 2 h, and (c) as in b, Sn-MCM-41(C) treated in air at 520 K for 2 h.

suggesting that a major part of tin is present as an isomorphous substituent for Si.

The sample with the largest tin content, Sn-MCM-41(D) (Si/Sn = 50), exhibits an intermediate IS value (−0.1 mm/s), between the previously considered −0.2 s and 0.0 mm/s values, the latter being characteristic of SnO_2 with octahedral coordination. Thus, it appears likely that the −0.1 mm/s IS value is due to the presence of both types of coordination, i.e., tetrahedral (framework substituted) and octahedral (extra-framework), in comparable amounts in sample Sn-MCM-41(D). A similar conclusion was also made from UV–vis studies. It is also worth mentioning that the QS value obtained for Sn-MCM-41(D) is the largest among the values obtained for the samples, attesting further to the presence of extra-framework SnO_2.

The comparison of $d \ln A/dT$ values is also worthy of consideration. Although the values scatter to a certain extent (which might also be partly attributed to differences in sample thickness, etc.), sample Sn-MCM-41(D) exhibits the lowest $d \ln(A_{300}/A_{77})/dT$ value, attesting to the strongest average Sn–O bond in this sample [the stronger the bond, the smaller the $d \ln A/dT$ value (31)]. Again, this feature can probably be attributed to the contribution of SnO_2 [which has a low $d \ln(A_{300}/A_{77})/dT$ value (31)].

Besides the IS = −0.2 mm/s value, sample Sn-MCM-41(C) exhibits the largest $d \ln A/dT$ value. This large value is attributed to the presence of isomorphically substituted tin to a large extent in the MCM-41 structure; thus, this sample was selected for further studies on the effects of reduction and oxidation treatments on the state of substituted Sn^{4+}. The treatment in a flow of hydrogen at 670 K resulted in partial reduction; more than a half of the Sn^{4+} was reduced to the Sn^{2+} state. The IS and QS parameters are close to those characteristic of the so-called red modification of SnO or those of hydroxo- complexes of Sn^{2+} (32). In addition, the $d \ln A/dT$ value obtained for the Sn^{2+} component is quite large. Thus, the Sn^{2+} component is probably present in a loosely bound form (e.g., in a hydroxylated state, forming Si–O–Sn^{2+}–OH groups).

The subsequent oxidation treatment in air at 520 K resulted in full reoxidation to the Sn^{4+} state. However, the original tetrahedral coordination does not appear to be restored, as suggested by the increase in IS and QS values (Table 3). Most probably SnO_2 is formed to a significant extent due to the redox treatment since the IS and QS values are shifted toward the characteristic values of this compound. Correspondingly, a decrease in the $d \ln(A_{300}/A_{77})/dT$ value of Sn^{4+} is also noted.

Finally, it is worth comparing the present Mössbauer data obtained on tin-containing MCM-41 with those obtained on medium-pore MFI and MEL and large-pore MTW tin silicalites (30). In general, similarities such as the presence of tetrahedrally coordinated Sn^{4+} and the reducibility of a certain amount of Sn^{4+} to Sn^{2+} in the structure (30) are noted. On the other hand, the MCM-41 structure exhibits a smaller ability to stabilize the Sn^{2+} state. For instance, all the Sn^{2+} was reoxidized to Sn^{4+} by the 520 K treatment in air, while in the other medium-pore zeolites the presence of Sn^{2+} was observed in significant amounts after similar treatments [this stabilization of Sn^{2+} was attributed to formation and stabilization of Si–O–Sn–O groups (30)]. In the MCM-41 structure the formation of similar groups is probably less pronounced, although the formation of hydroxylated Si–O–Sn^{2+}–OH groups may occur after reducing treatments.

Catalytic Activity

Hydroxylation. The Sn-MCM-41 samples possess selective oxidation properties when peroxides are used as oxidants. Hydroxylation of phenol and 1-naphthol was carried out over the four Sn-MCM-41 samples. For comparison, the reactions were also carried out over Sn-impregnated MCM-41 and Si-MCM-41. The inactivity of the Sn-free material (Si-MCM-41) suggests that Sn ions are responsible for activity. This is also confirmed by the increase in conversion with increase in Sn content of the samples (Tables 4 and 5). In both the hydroxylation reactions the activity of the Sn-impregnated MCM-41 was much less than those of the Sn-MCM-41 samples (Tables 4 and 5). This is probably due to the larger activity of the Sn^{4+} incorporated into the framework than the impregnated Sn species. Interestingly, it is noted that the turnover numbers (TONs; number of molecules converted per Sn atom; Tables 4 and 5) decrease with increasing Sn content. If all the Sn ions were equally active and monoatomically dispersed in the samples, one

TABLE 4

Activity of the Samples in the Hydroxylation of Phenol[a]

Sample	Phenol conversion (mol%)	H_2O_2 selectivity (mol%)	TON[b]	Product distribution (mass %)[c]		
				PBQ	CAT	HQ
Sn-MCM-41(A)	14.8	50.0	170.5	30.0	55.4	14.6
Sn-MCM-41(B)	17.4	55.8	150.5	26.4	57.4	16.2
Sn-MCM-41(C)	20.2	65.3	110.3	25.2	57.5	17.3
Sn-MCM-41(D)	22.8	72.3	64.8	23.8	57.8	18.4
Sn-impregnated MCM-41	1.0	3.9	3.4	50.0	25.0	25.0
Si-MCM-41	No detectable activity					
Sn-silica gel	1.3	5.2	4.4	55.2	24.8	20.0
SnO_2	0.5	2.0	0.1	53.5	24.3	22.2
VS-2 (SI/V = 79)[d]	25.8	58.7	133.7	2.3	55.5	42.2

[a] Reaction conditions: phenol = 1 g; phenol/H_2O_2 = 3; catalyst = 0.1 g; solvent (water) = 10 g; reaction time = 24 h.

[b] Turnover number (number of molecules of phenol converted per atom of Sn in 24 h).

[c] PBQ, *para*-benzoquinone; CAT, catechol; HQ, hydroquinone.

[d] Data of Rao *et al.* (34).

TABLE 5

Activity of the Samples in the Hydroxylation of 1-Naphthol[a]

Sample	1-Naphthol conversion (mol%)	H_2O_2 selectivity (mol%)	TON[b]	Product distribution (wt%)		
				1,4-Naphthoquinone	1,4-Dihydroxynaphthalene	1,2-Dihydroxynaphthalene
Sn-MCM-41(A)	14.2	40.0	53.4	88.0	7.7	4.3
Sn-MCM-41(B)	15.3	42.3	43.2	84.3	11.1	4.6
Sn-MCM-41(C)	17.1	46.9	30.5	83.0	12.3	4.7
Sn-MCM-41(D)	18.9	55.6	17.5	82.1	13.1	4.8
Sn-impregnated MCM-41	1.0	4.5	1.1	50.0	50.0	—
Si-MCM-41				No detectable activity		
Sn-silica gel	1.2	2.8	1.3	58.3	25.0	16.7
SnO_2	0.5	1.2	0.03	60.0	20.0	20.0

[a] Reaction conditions: 1-naphthol = 0.5 g; 1-naphthol/H_2O_2 (mole ratio) = 1.5; catalyst = 0.1 g; solvent (acetonitrile) = 10 g; temperature = 353 K; reaction time = 24 h.

[b] Turnover number (number of molecules of 1-naphthol converted per atom of Sn in 24 h).

would expect a constancy in the TONs for all the samples. The possible explanation for the decrease is that more than one type of Sn species is present in the samples, and the proportion of the less active Sn species increases with Sn content in the samples (samples A to D). Both UV–vis and Mössbauer studies suggest the presence of octahedrally coordinated Sn (besides Sn in tetrahedral coordination) in samples containing more Sn. Part of the Oh Sn could also exist as poorly dispersed SnO_2. The TON values are smaller for 1-naphthol than for phenol despite the larger amount of H_2O_2 used for hydroxylation of the former due to the greater difficulty of the reaction. The major product in naphthol hydroxylation is 1,4-naphthoquinone produced from the subsequent oxidation of the primary 1,4-dihydroxy product. In the case of phenol, the activities of the Sn-MCM-41 samples are similar to those reported for VS-2 by earlier workers (33, 34). For example, a TON of 133 was reported by Rao and Ramaswamy (34) for VS-2 with Si/V = 79, comparable to the value (110) observed by us for Sn-MCM-41(C) with Si/Sn = 82. Though the ratios of the yields of the *p*/*o* products ((PBQ + HQ)/CAT) is similar (∼1) to those reported for titano- and vanadosilicates (34, 35) in aqueous medium, more benzoquinone is formed over the Sn-MCM-41 samples, suggesting the deeper oxidation ability of the active Sn species.

Epoxidation. The Sn-MCM-41 samples were also active in the epoxidation of norbornene with tertiary butyl hydroperoxide (TBHP) (Table 6). The reaction was nearly complete after 10 h. Continuing the reaction up to 24 h increased the conversion only marginally [28.2% at 10 h and 29.7% at 24 h in the case of Sn-MCM-41(A)]. This is attributed to the near exhaustion of the peroxide after 10 h through consumption in the reaction and decomposition. Similar results were also obtained over the other samples. Again the TON values decrease with increase in the Sn

TABLE 6

Activity of Samples in Epoxidation of Norbornene over Sn-MCM-41[a]

Sample	Reaction time (h)	Norbornene conversion (mol%)	TON[b]	Product distribution			
				exo-2,3-Epoxy norbornene	*endo*-2,3-Epoxy norbornene	*exo*- + *endo*-norborneol	Others
Sn-MCM-41(A)	4	10.5	15.1	86.0	4.0	4.7	5.3
	10	28.2	16.2	85.3	3.8	4.5	6.4
	24	29.7	7.1	78.2	3.3	11.6	6.9
Sn-MCM-41(B)	10	38.9	16.8	82.8	3.8	5.6	7.8
Sn-MCM-41(C)	10	45.6	12.7	80.3	4.2	6.0	9.5
MCM Sn–41(D)	10	47.2	6.7	78.0	6.3	6.8	8.9
Sn-impregnated MCM-41	10	2.0	0.3	71.6	6.9	13.0	8.5

[a] Reaction conditions: norbornylene = 0.5 g; norbornylene/TBHP (mole ratio) = 1.5; catalyst = 0.1 g; solvent (acetonitrile) = 10 g; temperature = 353 K.

[b] Turnover number (number of molecules of norbornene converted per atom of Sn per hour).

content of the samples. This was earlier attributed to the larger amount of the less active Oh Sn species in samples with more Sn. The ratio of TONs (at 24 h) of samples D and A (TON of D/TON of A) is about 0.41 for the epoxidation, which is comparable to the values of 0.38 and 0.33 for the hydroxylation of phenol and naphthol, respectively (Tables 4 and 5). The reasonable similarity in values could suggest that the relative activities of the different Sn sites are similar for the different reactions. Analysis of Sn-MCM-41(D) after the reaction (and after calcination at 823 K) revealed no detectable loss of Sn during the reaction (Si/Sn was 42 both before and after the reaction). The S_{BET} (1000 m^2/g) and average pore size of the used catalyst were also similar.

CONCLUSIONS

Sn^{4+} ions can be incorporated into the framework of MCM-41 by hydrothermal synthesis methods. UV–vis and Mössbauer studies suggest that the ions are present mostly in a tetrahedral environment, though the samples with higher Sn content contain octahedral Sn^{4+} ions also. Mössbauer studies reveal that the ions undergo reversible redox transformation on treatment with H_2 (at 670 K) or air (at 520 K). The absence of significant broadening of the ^{13}C signal of the $=N-CH_2$ and $=N-CH_3$ groups reveals the absence of a charged framework, suggesting the incorporation of Sn as Sn^{4+} ions. The ^{29}Si NMR spectra reveal the presence of large amounts of Q_3 species [$Si(OSi)_3OH$]; the species are probably mainly present at the surface of the pores. Sn-MCM-41 is a good catalyst for the hydroxylation of phenol and 1-naphthol and the epoxidation of norbornene.

ACKNOWLEDGMENT

K. Chaudhari thanks CSIR, New Delhi, for a research fellowship.

REFERENCES

1. Kresge, C. T., Leonowicz, M. E., Roth, W. J., and Vartuli, J. C., U.S. Patent 5098684 (1992).
2. Kresge, C. T., Leonowicz, M. E., Roth, W. J., Vartuli, J. C., and Beck, J. S., *Nature* **359**, 710 (1992); Beck, J. S., Vartuli, J. C., Roth, W. J., Leonowicz, M. W., Scmitt, K. D., Chu, C. T. W., Olson, D. H., Sheppard, E. W., McCullan, S. B., Higgins, H. B., and Shlenker, J. S., *J. Am. Chem. Soc.* **114**, 10834 (1992).
3. Tanev, P. T., Chibwe, M., and Pinnavaia, T. J., *Nature* **368**, 321 (1994).
4. Corma, A., Navarro, M. T., and Perez-Pariente, J., *J. Chem. Soc. Chem. Commun.*, 147 (1994).
5. Gontier, S., and Tuel, A., *Stud. Surf. Sci. Catal.* **97**, 157 (1995).
6. Reddy, K. M., Moudrakovski, I., and Sayari, A., *J. Chem. Soc. Chem. Commun.*, 1059 (1994).
7. Reddy, J. S., and Sayari, A., *J. Chem. Soc. Chem. Commun.*, 2231 (1995).
8. Park, D. H., Cheng, C.-F., and Klinowski, J., *J. Mater. Chem.* **7**(1), 159 (1997).
9. Das, T. K., Chaudhari, K., Chandwadkar, A. J., and Sivasanker, S., *J. Chem. Soc. Chem. Commun.*, 2495 (1995).
10. Ulagappan, N., and Rao, C. N. R., *J. Chem. Soc. Chem. Commun.*, 1047 (1996).
11. Das, T. K., Chaudhari, K., Nandanan, E., Chandwadkar, A. J., Sudalai, A., Ravindranathan, T., and Sivasanker, S., *Tetrahedron Lett.* **38**, 3631 (1997).
12. Jones, D. J., Jimenez-Jimenez, J., Jimenez-Lopez, A., Maireles-Torres, P., Olivera-Paster, P., Rodriguez-Castellon, E., and Roziere, J., *Chem. Commun.*, 431 (1997).
13. Skeels, G. W., and Flanigen, E. M., *Stud. Surf. Sci. Catal.* **49A**, 331 (1989).
14. Skeels, G. W., and Flanigen, E. M., U.S. Patent Appl. 133 372 (1987).
15. Skeels, G. W., and Flanigen, E. M., European Patent 321 177 (1989).
16. Vaughan, D. E. W., and Rice, S. B., U.S. Patent 4 933 161 (1990) assigned to Exxon.
17. Dwyer, F. G., and Jenkins, E. E., U.S. Patent 3 941 871 (1976) assigned to Mobil.
18. Corcoran, E. W., Jr., and Vaughan, D. E. W., U.S. Patent 5 192 519 (1993) assigned to Exxon.
19. Mal, N. K., and Ramaswamy, A. V., *J. Mol. Catal.* **105**, 149 (1996).
20. Mal, N. K., Ramaswamy, V., Ganapathy, S., and Ramaswamy, A. V., *Appl. Catal. A* **125**, 233 (1995).
21. Borade, R. B., and Clearfield, A., *Catal. Lett.* **31**, 267 (1995).
22. Gregg, S. J., and Sing, K. S. W., *in* "Adsorption, Surface Area and Porosity," Chap. 4. Academic Press, London, 1982.
23. Barrett, E. P., Joyner, L. G., and Halenda, P. H., *J. Am. Chem. Soc.* **73**, 373 (1951).
24. Beck, J. S., Chu, C. T. W., Kresge, C. T., Leonowicz, M. E., Roth, W. J., and Vartuli, J. C., U.S. Patent 11390 (1991).
25. Cambler, M. A., Corma, A., and Perez-Pariente, J., *J. Chem. Soc. Chem. Commun.*, 147 (1993).
26. Thangaraj, A., Kumar, R., Mirajkar, M. P., and Ratnasamy, P., *J. Catal.* **130**, 1 (1991).
27. Sen, T., Chatterjee, M., and Sivasanker, S., *J. Chem. Soc. Chem. Commun.* **5**, 207 (1995).
28. Caravlho, W. A., Paula, B. V., Wallau, M., and Schuchardt, U., *Zeolites* **18**, 408 (1997).
29. Fejes, P., Nagy, J. B., and Vanko, Gy., *Appl. Catal. A* **145**, 155 (1996).
30. Lazar, K., Szeleczky, N. K., Mal, N. K., and Ramaswamy, A. V., *Zeolites* **19**, 123 (1997).
31. Parish, R. V., *in* "Mössbauer Spectroscopy Applied to Inorganic Chemistry" (G. J. Long, Ed.), Vol. 1, p. 527. Plenum, New York, 1984.
32. Greenwood, N. N., and Gibb, T. C., "Mössbauer Spectroscopy," p. 388. Chapman & Hall, London, 1971.
33. Ramaswamy, A. V., and Sivasanker, S., *Catal. Lett.* **22**, 239 (1993).
34. Rao, P. R. H. P., and Ramaswamy, A. V., *Appl. Catal. A* **93**, 123 (1993).